



Investigation of plasma-functionalized multiwalled carbon nanotube film and its application of DNA sensor for *Legionella pneumophila* detection

Eun Jin Park^a, Jun-Yong Lee^a, Jun Hyup Kim^a, Cheol Jin Lee^b, H. Stanley Kim^c, Nam Ki Min^{a,d,*}

^a Department of Biomicrosystem Technology, Korea University, Seoul 136-701, Republic of Korea

^b School of Electrical Engineering, Korea University, Seoul 136-701, Republic of Korea

^c Department of Medicine, Korea University, Seoul 136-705, Republic of Korea

^d Department of Control and Instrumentation Engineering, Korea University Sejong Campus, Chungnam 339-700, Republic of Korea

ARTICLE INFO

Article history:

Received 23 March 2010

Received in revised form 14 May 2010

Accepted 17 May 2010

Available online 24 May 2010

Keywords:

Multiwalled carbon nanotubes

Oxygen plasma treatment

Electrochemical analysis

DNA detection

Legionella pneumophila

ABSTRACT

A novel multiwall carbon nanotube (MWCNT) electrode functionalized with oxygen plasma treatment was prepared and characterized, and its DNA sensing ability for *Legionella pneumophila* (*L. pneumophila*) detection was examined using electrochemical measurement. A well-patterned MWCNT working electrode (WE) on a Pt track was fabricated using photolithography, transfer methods and an etching technique. The MWCNT WE was functionalized by oxygen plasma treatment prior to applying for DNA sensor. The surface morphology of the plasma-functionalized MWCNT (pf-MWCNT) WEs were observed by scanning electron microscope (SEM) and the change of chemical composition was characterized by X-ray photoelectron spectroscopy (XPS), and electrochemical measurements were performed using CV with ferricyanide/ferricyanide redox couple. Effective areas of working electrodes were calculated to be 0.00453 cm² for pristine MWCNT electrode and 0.00747–0.00874 cm² for pf-MWCNT electrodes with different plasma treatment times. Differential pulse voltammetry (DPV) was carried out in methylene blue solution for DNA sensing. The pf-MWCNT based DNA sensor was successfully operated in a target concentration range of 10 pM to 100 nM and had a lower detection limit than a pristine MWCNT based DNA sensor.

© 2010 Elsevier B.V. All rights reserved.

1. Introduction

Carbon nanotubes (CNTs) have been widely studied, especially in biosensor applications, since Iijima first reported his findings of them in 1991 [1]. In recent years, there have been numerous studies of CNT as an electrode material in electrochemical biosensors due to their large surface area and excellent electrical property [2,3]. Many experimental results have shown that defects or structural changes in the CNT surface affect the electrocatalytic activity of the CNT [4,5]. These unique properties can be used to develop electrochemical sensors and biosensors with a lower analytical voltage and a higher response current [2,6].

Most studies of CNT electrodes have been limited to composite electrodes with various polymers [3,7–10], metallic nanoparticles [10–14], or to CNT modified on universal electrodes such as indium tin oxide (ITO) [11], glassy carbon electrode (GCE) [4,15] and gold

electrode [16]. These composite electrodes or CNT modified electrodes could have many fabrication steps and a lack of uniformity in electrochemical properties. Therefore, it is almost impossible to mass-produce CNT electrodes due to complicated preparation requirements. In this study, MWCNT WEs were fabricated using photolithography, lift-off and plasma etching techniques, and all fabrication procedures were performed on a wafer scale to make uniform electrodes. We were able to obtain MWCNT WEs successfully without any other additives such as polymers and nanoparticles. They have high uniformity and good potential for various commercial applications for chemical and biosensors.

Since CNTs are insoluble and difficult to handle, some treatments such as acid treatment, electrochemical treatment, and plasma treatment have been frequently used for many purposes [17] including removal of impurities, improving electrical properties and various functionalizations. Among the surface functionalization techniques of CNT, oxidation is probably the most widely studied [13] and plasma functionalization, i.e. generation of surface-bound functional groups without deposition of a coating, is considered a promising solution to enhance the reactivity of CNTs [18]. There have been many studies of plasma treatments on CNTs with several variables such as bias power, flow rate, and different gases. In our previous work [19], a sensitive biosensor

* Corresponding author at: Department of Biomicrosystem Technology, Korea University, Seoul 136-701, Republic of Korea. Tel.: +82 2 3290 3991; fax: +82 2 925 2296.

E-mail addresses: parkeunjin@korea.ac.kr (E.J. Park), lord_junyong@naver.com (J.-Y. Lee), anycall6950@naver.com (J.H. Kim), cjlee@korea.ac.kr (C.J. Lee), hstanleykim@korea.ac.kr (H.S. Kim), nkmin@korea.ac.kr (N.K. Min).

was fabricated using oxygen plasma-treated MWCNT film in a simple custom-made plasma chamber, which was just able to control the bias power, flow rate, and treatment time. As described in the previous work, oxygen plasma treatment on MWCNT WEs produced two effects at the same time: the strong energy of plasma produces numerous defects in the MWCNTs, and the dissociated oxygen molecules by plasma are able to react with the MWCNT defects that are functionalized with oxygen-containing chemical groups [17–19]. Therefore, oxygen plasma treatment could give the MWCNT a high electrocatalytic property, and introduce many functional groups to attach amine-moieties of various biomolecules covalently.

Legionella pneumophila (*L. pneumophila*) is a contaminant of man-made water systems including cooling towers of large buildings and waterworks, and is a major cause of legionellosis, a respiratory infection that may give rise to restricted outbreaks [20,21]. The macrophage infectivity potentiator (*mip*) is a conserved region in *L. pneumophila*, and is divergent in other legionellae [21–27]. Therefore, the *mip* gene was selected as the detection target sequence in this work.

Many researchers have studied *L. pneumophila* detection with the *mip* gene over the past two decades [22]. Most studies were based on PCR [24], and more recently real-time PCR [21,25–27] and other optical detection methods [28]. These methods are time-consuming, labor-intensive, and require expensive instrumentation [29]; therefore, simplified methods suitable for rapid analysis are needed. We proposed electrochemical analysis for *L. pneumophila* detection with the pf-MWCNT electrode. As many studies have shown, the electrochemical methods have many advantages compared to optical methods including simple sample preparation procedures, rapid measurement time, low cost and ease of miniaturization for portable devices [2,30].

Methylene blue (MB), an organic dye that belongs to the phenothiazine family, is a well-known hybridization indicator of DNA due to its association with the free guanine bases of single-stranded DNA (ssDNA) [29]. The affinity interaction between MB and ssDNA occurs quickly and generates a marked electrochemical signal [31]. Thus, MB was used as the hybridization indicator in this work.

This study proposes a method for the preparation and the characterization of well-patterned MWCNT as a sensing electrode and the application of an electrochemical DNA sensor for *L. pneumophila* detection.

2. Materials and methods

2.1. Materials

MWCNTs were synthesized using the catalytic chemical vapor deposition method. The details of the synthesis process and the relevant conditions were described in our previous paper [32]. As described previously, the MWCNT synthesis procedure included acid treatment, and the surface of the MWCNT was slightly oxidized. Therefore, the pristine MWCNT in this work has a small amount of oxidative surface.

The sequences for *L. pneumophila* detection were selected from the *mip* gene, which is a well-known *L. pneumophila*-specific sequence. The 5-end of the DNA probe was modified with amine ($-NH_2$) moiety to make the probe attach onto the oxidative surface of MWCNT WEs. All oligonucleotides employed in this study were synthesized by Bioneer[®] (Daejeon, Korea) and their base sequences are as follows:

Probe sequence: 5'-NH₂-TAG CTA CAG ACA AGG ATA AGT-3'

Complementary sequence (target): 5'-ACT TAT CCT TGT CTG TAG CTA-3'

Non-complementary sequence: 5'-ATG CGA GTG CAG TTG CAG TAG-3'

Methylene blue (MB) was obtained from Junsei Chemical (Japan). 1-Ethyl-3-[3-dimethylaminopropyl]carbodiimide hydrochloride (EDC); N-hydroxy-sulfo-succinimide-ester (NHSS); 3-mercaptopropionic acid (MPA); potassium chloride (KCl); potassium ferricyanide ($K_3[Fe(CN)_6]$); dimethylformamide (DMF); aluminum oxide membrane (Whatman); Tris-EDTA buffer (TE buffer, pH 8.0); and all organic solvents were purchased from Sigma-Aldrich (St. Louis, MO) and were used without further purification.

All oligonucleotide stock solutions were prepared and diluted using TE buffer.

2.2. Apparatus

Oxygen plasma treatment of the MWCNTs was performed in a custom-made chamber. To observe the surface of MWCNT electrodes, images were taken with a scanning electron microscope (S-4300, Hitachi) and an atomic force microscope (XE-100, PSIA). The chemical composition of the MWCNT surface was characterized by X-ray photoelectron spectroscopy (K-Alpha, Thermo Electron). Electrochemical analyses were performed with a potentiostat (263A, Perkin Elmer) at room temperature with a conventional three-electrode system: working electrode (WE), the MWCNT film; counter electrode (CE), patterned Pt; reference electrode (RE), screen printed Ag/AgCl.

2.3. Fabrication of MWCNT working electrodes

To construct the three-electrode system, a Pt track was patterned on a Pyrex[®] glass wafer using photolithography, sputtering (DC magnetron sputter, INOSTECK Inc., Korea, 150 W, 30 sccm of Ar gas, 5 mPa) and lift-off techniques. Patterned Pt was used as the CE and the Ag/AgCl RE was fabricated on the Pt track using the screen printing method. MWCNT WEs were prepared with the following procedures [32]: a homogeneous MWCNT suspension was obtained by tip-sonication in DMF for 30 min. The MWCNT/DMF mixture was centrifuged for 30 min, the bottom solution was separated from the top solution. The bottom solution was filtered with an aluminum oxide membrane (the pore size was 0.45 μ m) under a vacuum condition. Then, the filtered MWCNTs were transferred onto the previously patterned Pt track. Finally, photolithography and plasma etching technique were performed to produce a well-confined MWCNT WE of 1.4 mm diameter.

2.4. MWCNT functionalization by O₂ plasma

In order to introduce oxygen-containing functional groups such as $-C-O$, $-C=O$ and $-COO$, MWCNT WEs were treated with O₂ plasma. The treatment was carried out in a custom-made chamber with the following parameters: power 20 W; flow rate 10 sccm; and exposure times of 10, 15, 30, and 60 s. In our previous work [19], we showed that CVs of MWCNT electrodes revealed that the peak currents increased in accordance with increases in plasma power from 0 to 60 W. The MWCNT films in this study were thinner and the films were etched over 30 W; therefore, a power of 20 W was chosen for this work.

2.5. Probe DNA immobilization and hybridization

The pf-MWCNT WEs were chemically activated with an aqueous solution containing 75 mM EDC and 15 mM NHSS for 2 h. For probe DNA immobilization, the pf-MWCNTs were immersed into 200 μ L of TE buffer solution containing 1 μ M probe oligonucleotide

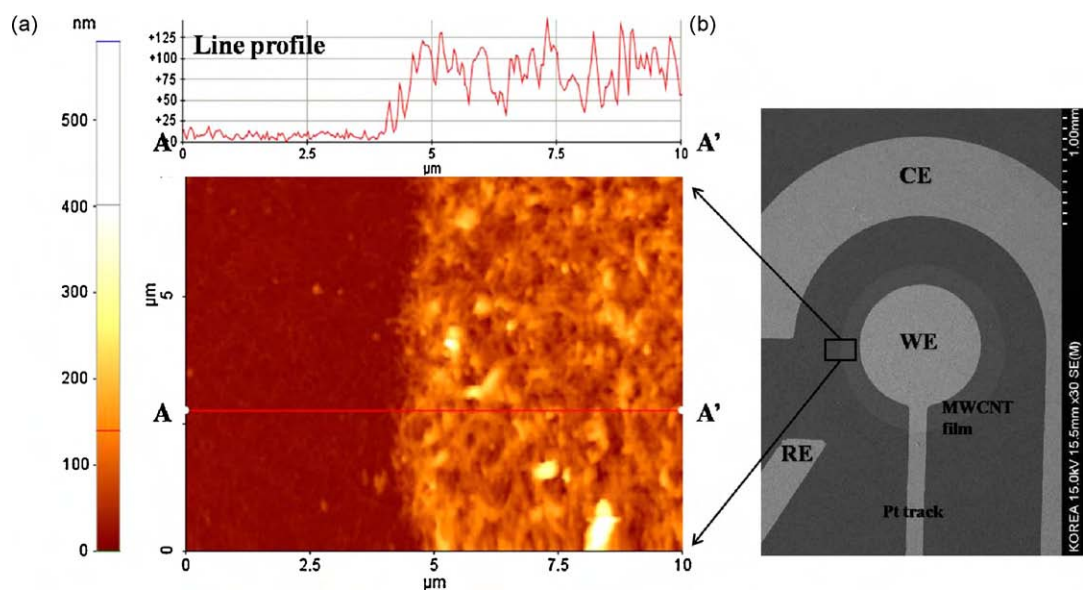


Fig. 1. MWCNT electrode. (a) AFM image of MWCNT WE and line profile of WE and glass substrate (10 μm × 10 μm scale). (b) Configuration of three-electrode system (SEM, 30×).

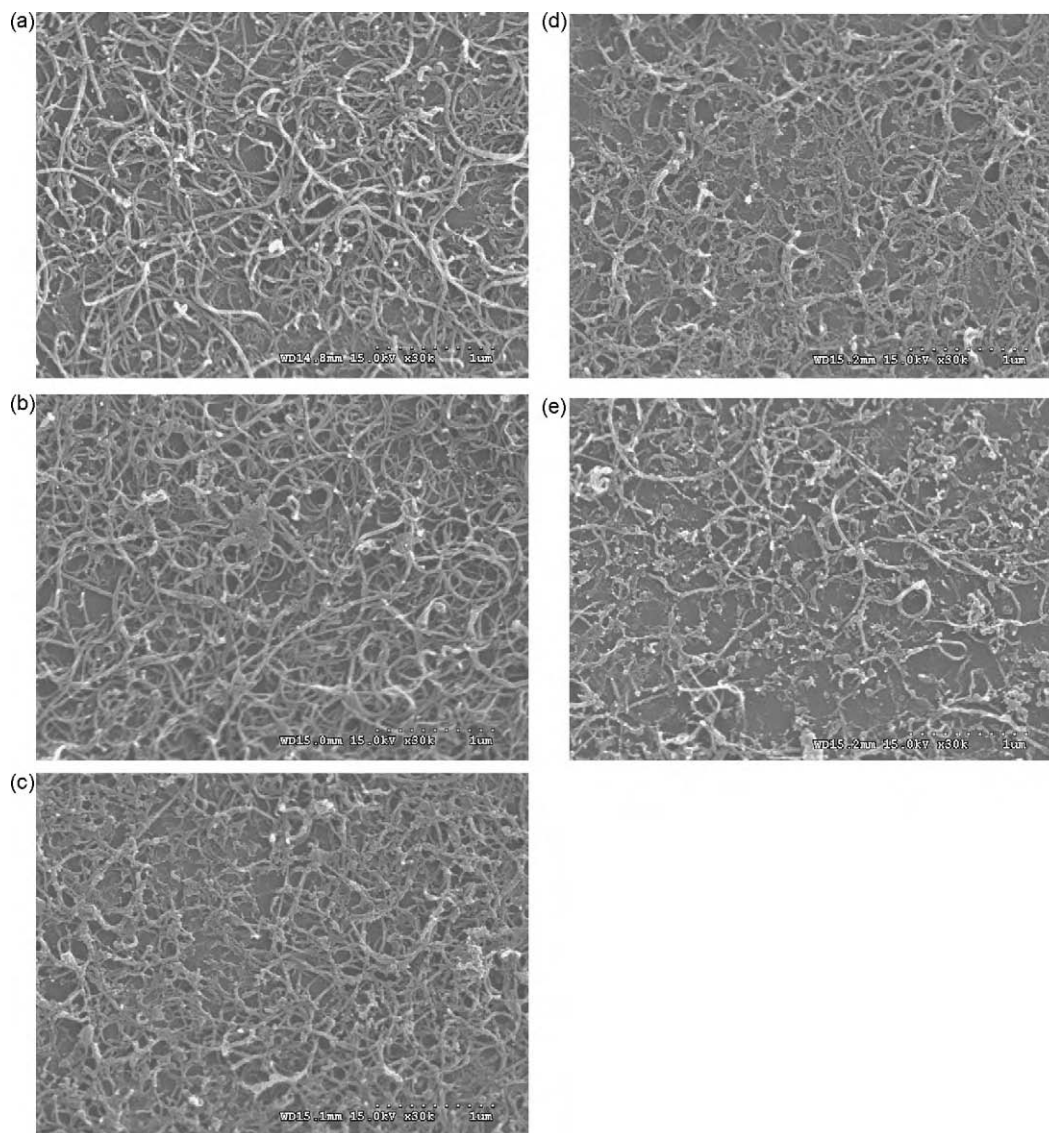


Fig. 2. SEM images of MWCNT working electrodes with different plasma exposure times. (a) Pristine, (b) 10 s, (c) 15 s, (d) 30 s and (e) 60 s.

for 2 h. Then, the electrodes were washed with TE buffer to remove unbound oligonucleotides. DNA hybridization was performed by dropping 4 μl of target DNA solution onto a probe DNA modified pf-MWCNT electrode. To maximize hybridization efficiency and sensor response, the hybridization proceeded for 30 min, followed by thoroughly washing the unhybridized target DNA away from the MWCNT WE surfaces. The concentration range of target DNA was 10 pM to 100 nM. All experiments were performed at room temperature ($25 \pm 1^\circ\text{C}$).

2.6. Electrochemical investigation of pf-MWCNT electrodes and DNA sensors for *L. pneumophila* detection

In electrochemical experiments, CVs were carried out in 3 M potassium chloride (KCl) aqueous solution containing 10 mM potassium ferricyanide ($\text{K}_3[\text{Fe}(\text{CN})_6]$) with scan rates of 10, 20, 50, 100, 200, and 300 mV/s. Differential pulse voltammetry (DPV) was performed in 75 mM phosphate buffer including 20 μM MB with potential from 0 to -0.5 V , a pulse amplitude of 50 mV, a pulse width of 50 ms, a pulse period of 200 ms and a scan rate of 10 mV/s. For effective intercalation of MB, all electrodes used for DPV were immersed in MB solution for 10 min before measurement. The

bare WE, single-stranded DNA (ssDNA), and double-stranded DNA (dsDNA) used for the DPV measurement were examined under the same conditions.

3. Results and discussion

3.1. Characterization of the MWCNT electrode

3.1.1. Surface morphologies of MWCNT electrodes

Fig. 1 shows the well-confined MWCNT film on the substrate and three-electrode system including the MWCNT WE, Pt CE and Ag/AgCl RE (not shown in this picture). The line profile (AA') of the AFM image reveals that the thickness of the MWCNT film is about 100 nm, and the MWCNTs on the glass wafer were clearly etched except for the WE area. The MWCNT WEs were also measured with different plasma treatment times as shown in Fig. 2. The simple tubular-shape of the pristine MWCNTs gradually lost their own structures with increased treatment time, and they aggregated themselves. As the treatment time increased, the degree of deformation progressed due to the existence of defect sites on the MWCNT surface and bonding with oxygen molecules on the surface.

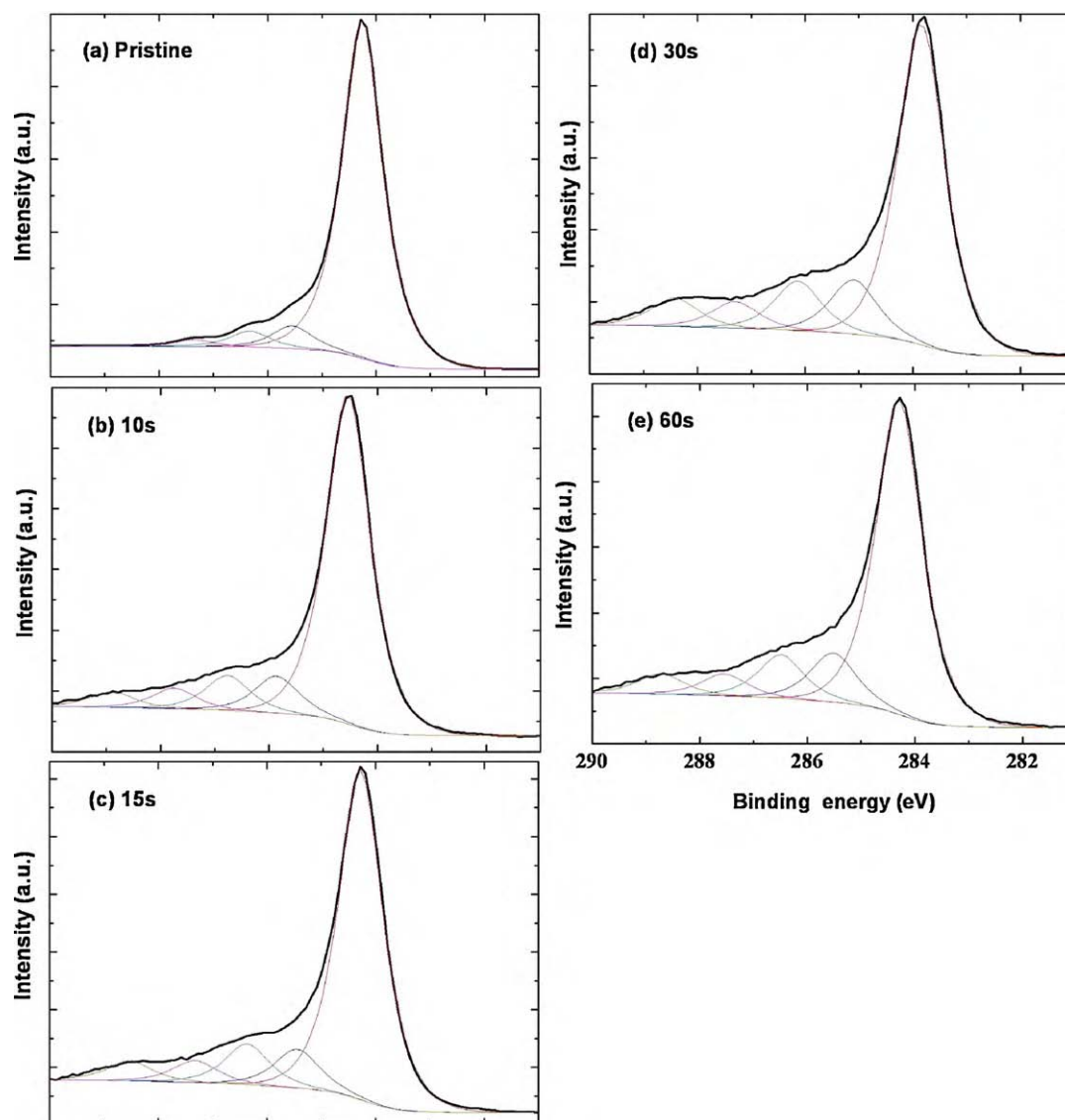


Fig. 3. C1s XPS spectra of (a) pristine, (b)10s, (c)15s, (d)30s and (e)60s.

Table 1
Peak assignments of XPS C1s spectra.

Plasma treatment time on MWCNTs (s)	sp ²		sp ³		–C–O		>C=O		–COO		[COx]/[C]
	BE (eV)	%	BE (eV)	%	BE (eV)	%	BE (eV)	%	BE (eV)	%	%
0	284.25	88.0	285.54	6.0	286.33	4.3	287.36	1.7	–	–	6.4
10	284.54	75.3	285.86	8.5	286.77	8.1	287.74	4.7	288.9	16.3	19.4
15	284.27	72.7	285.45	8.6	286.37	9.0	287.32	5.4	288.53	18.7	23.1
30	283.84	66.9	285.1	11.3	286.14	10.3	287.3	5.5	288.43	21.8	27.8
60	284.29	69.8	285.52	11.0	286.49	9.7	287.55	4.9	288.73	19.1	23.7

3.1.2. XPS spectra of MWCNT electrodes

Fig. 3 shows the C1s core level photoemission spectra of plasma-treated MWCNTs with different plasma treatment times and the XPS peak assignments including peak positions (binding energy) and their percentages are summarized in Table 1. As shown in Fig. 3(a)–(e), the asymmetric peak was observed for all MWCNT films, centered at 284.24 ± 0.4 eV. The main peak at 284.24 ± 0.4 eV originates in both sp²-hybridized graphite-like carbon atoms and hydrogen-bound carbon atoms [13,17]. 285.5 ± 0.4 eV could be assigned to sp³-hybridized carbon atoms. These two peaks reveal carbon atoms without the presence of oxygen atoms. The other three peaks with higher BEs at 286.4 ± 0.4 , 287.5 ± 0.3 , and 288.6 ± 0.3 are considered to have originated in carbon atoms bound to one or more oxygen atom because electronegative oxygen atoms induce a positive charge on carbon atoms [17]. They can be assigned as –C–O (alcohol, ether), >C=O (ketone, aldehyde), and –COO (carboxylic acid, ester) species, respectively. The pristine MWCNT shows a dominant peak structure for C1s level at 284.25 eV, which corresponds to the untreated CNT surface. The pristine MWCNT also reveals other peaks assigned to –C–O, >C=O, and COO due to its partial oxidation by acid purification procedure [12,32]. However, the oxidative species were relatively small, representing a [COx]/[C] ratio of 6.4%. As summarized in Table 1, the oxidative species on MWCNTs were increased up to 30 s with plasma treatment time increases, and slightly decreased at 60 s suggesting that the surface of MWCNTs lost their intrinsic properties in chemical composition.

3.1.3. Cyclic voltammograms of MWCNT electrodes

To confirm electrocatalytic activity changes in the pf-MWCNT WEs, CV was performed in 3 M potassium chloride (KCl) aqueous solution containing 10 mM potassium ferricyanide ($K_3[Fe(CN)_6]$) with a scan rate of 100 mV/s. The CV results are shown in Fig. 4(a) and their peak currents (using baseline) are plotted versus plasma treatment times in Fig. 4(b). All CVs, even in pristine MWCNT electrode, revealed typical current–voltage curves at all electrodes. The peak potential value of the pristine MWCNT electrode reached 320.2 mV and the values of 10, 15, 30, and 60 s pf-MWCNT electrodes were less at 316.9, 311.7, 312.9, and 312.9 mV, respectively. CVs of the Pt track itself of WE were also measured for comparison, and its peak potential was 324.7 mV at a scan rate of 100 mV/s. The peak-to-peak separation (anodic peak potential–cathodic peak potential) values were 73, 72, 74 and 73 mV at pf-MWCNTs, while the value was 86 mV at the pristine MWCNT electrode (the peak-to-peak separation of Pt track was 84 mV). These results indicate that the electrochemical reaction happened in a more reversible matter at pf-MWCNT electrodes [30]. The peak currents of pf-MWCNTs increased in response to treatment times up to 30 s, and then, the values were saturated. CV data indicates that the electrocatalytic activity of plasma-functionalized MWCNTs significantly increased depending on the increase in O₂ plasma treatment time due to the presence of some oxygen-containing functional groups on the pf-MWCNT surface, in good agreement with the XPS results.

To validate the electrochemical property of the MWCNT electrode, the effective WE area was determined using CV at different

scan rates and employing a ferricyanide/ferricyanide redox couple. The relationship between the peak current and the square root of the scan rate is shown in Fig. 5(a). The peak currents depend linearly on the corresponding square root of the scan rate with high regression coefficients (R^2 values are shown in Table 2). The dependency indicates that a mass transport process has occurred in the oxidation process by diffusion [15]. Effective area (A_{eff}) of MWCNT electrode was calculated using the following equation [30]:

$$i_{pc} = (2.69 \times 10^5) n^{3/2} A D_0^{1/2} C_0^* \nu^{1/2}$$

where i_{pc} represents the peak current (A), n is the charge transfer number ($n = 1$), A is the surface area of working electrode (cm^2), D_0 is the diffusion coefficient ($7.6 \times 10^{-6} \text{ cm}^2/\text{s}$), C_0 is the bulk concentration of redox species (mol/L), and ν is the scan rate (V/s).

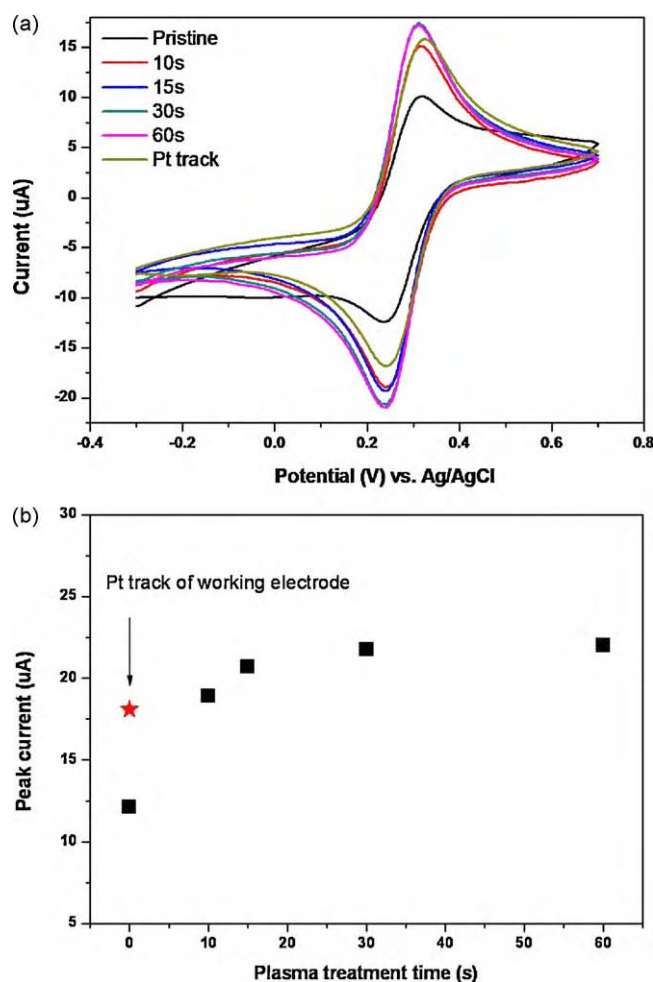


Fig. 4. Cyclic voltammograms of MWCNT WEs and Pt track without MWCNTs. CVs of 0–60 s plasma-treated MWCNT WEs and Pt track, and (b) their anodic peak current. CVs were carried out in 3 M KCl aqueous solution containing 10 mM $K_3[Fe(CN)_6]$ with a scan rate of 100 mV/s.

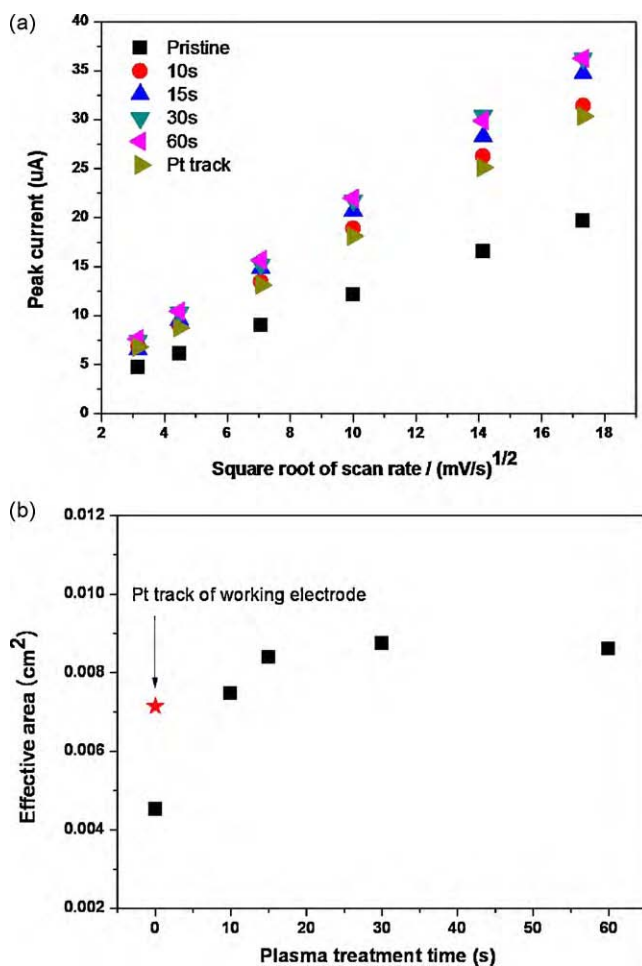


Fig. 5. Relationship between the square root of scan rates and (a) the anodic peak currents of MWCNT WEs and Pt track, and (b) the effective areas of them. CVs were measured in 3 M KCl aqueous solution containing 10 mM $K_3[Fe(CN)_6]$ with scan rates of 10, 20, 50, 100, 200 and 300 mV/s.

The calculation results are shown in Table 2 and Fig. 5(b). After 30 s plasma treatment, the pf-MWCNT WEs were found to have a much higher peak current and a effective area about 1.9 larger than that of a corresponding pristine MWCNT. The surface properties of pf-MWCNT WEs were affected significantly by oxygen plasma treatment, due to the presence of oxygen-containing defects at the surface of pf-MWCNTs. The A_{eff} of 1.0 mm diameter-Pt track was 0.00714 cm². Although the A_{eff} of Pt track was larger than that of pristine SWCNT WE (0.00453 cm²), the pf-SWCNT WEs have larger A_{eff} value than Pt track as well as pristine SWCNT WE. Moreover, Pt electrode is not able to be a sensing electrode itself since Pt is a noble metal and is hard to functionalize with other chemicals, while CNTs were easily functionalized with oxygen plasma treatment.

Table 2

Effective areas of MWCNT electrodes and Pt track calculated from CV results.

Plasma treatment time (s)	Slope ^a ($i_{pc}/\nu^{1/2}$)	R^2 ^b	A_{eff} ^c (cm ²)
0	1.0641	0.9996	0.00453
10	1.7524	0.9997	0.00747
15	1.9692	0.9994	0.00839
30	2.0518	0.9994	0.00874
60	2.0178	0.9997	0.00860
Pt track (1.0 mm diameter)	1.6758	0.9999	0.00714

^a Relationship between the square root of scan rates and peak current.

^b Regression coefficient (degree of linear relationship).

^c Effective area of working electrode area.

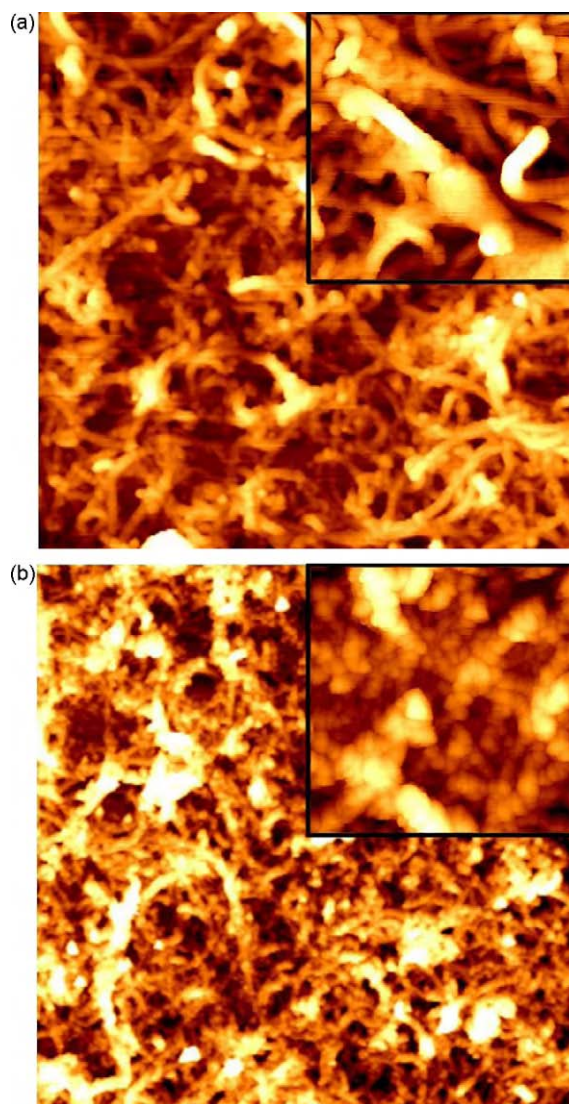


Fig. 6. AFM images of oligonucleotide immobilization on MWCNT WEs. Immobilization on (a) pristine and (b) 30 s plasma-treated MWCNT WE. Both were measured in 5 $\mu\text{m} \times 5 \mu\text{m}$ and inserted images were in 1 $\mu\text{m} \times 1 \mu\text{m}$.

3.2. Electrochemical performance of a pf-MWCNT WE based DNA sensor

According to XPS and CV results, the plasma treatment time on MWCNTs was fixed at 30 s for DNA sensor application. Fig. 6 shows AFM images of probe DNAs on a pristine WE and pf-MWCNT WE for a 30 s treatment time. The MWCNTs shown in Fig. 6(b) were uniformly covered with small molecules; probe DNA whereas Fig. 6(a) shows MWCNTs have their own structure. These results indicate that many oxygen-containing functional groups were effectively induced on the MWCNTs by oxygen plasma treatment, and that amine modified probes were uniformly immobilized on pf-MWCNTs.

DNA hybridization with a complementary target was detected by differential pulse voltammetry (DPV) in 20 μM MB solution [31]. MB has a strong affinity for the free guanine base present in ssDNA and it can act as a redox material in an electrochemical reaction. Fig. 7(a) reveals the DPV curves of MB at the bare pf-MWCNT electrode, probe DNA immobilization and non-complementary DNA on the DNA sensor. The DPV signal of MB was decreased after probe DNA immobilization, indicating that the free MB molecules in bulk solution were dominant than MB attached in ssDNA. As expected,

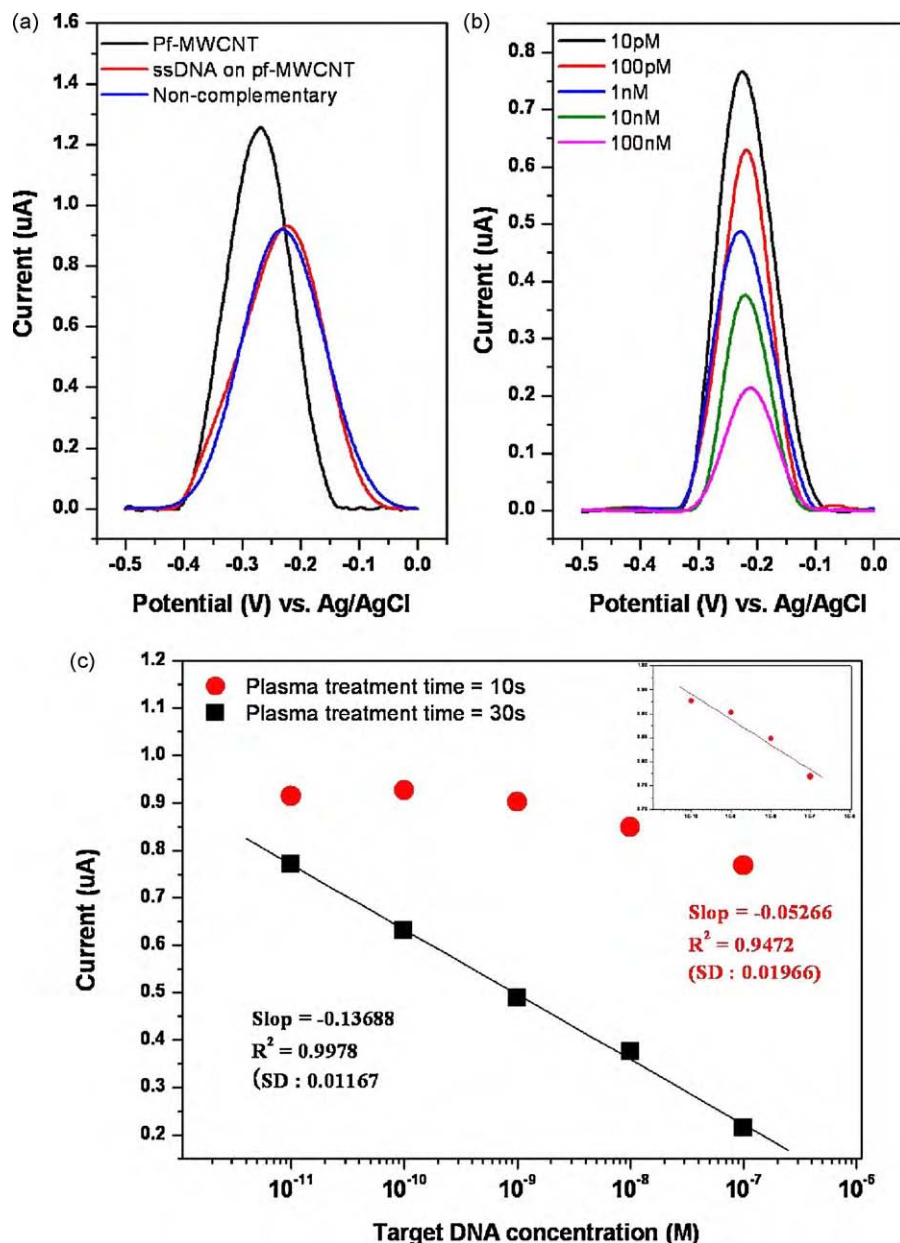


Fig. 7. Differential pulse voltammograms of pf-MWCNT based DNA sensor for *L. pneumophila* detection. (a) DPVs of pf-MWCNT, probe DNA immobilization on pf-MWCNT, and after hybridization with non-complementary target. (b) DPVs from 10 pM to 100 nM of target DNA concentration. (c) Calibration curves of pf-MWCNT based DNA sensors. Black rectangles indicate a 30 s pf-MWCNT based DNA sensor, and red circles indicate a 10 s pf-MWCNT based DNA sensor. The inserted graph shows the calibration curve of a 10 s pf-MWCNT based DNA sensor with 100 pM detection limit, while the detection limit is 10 pM in the 30 s pf-MWCNT based DNA sensor. (For interpretation of the references to color in this figure caption, the reader is referred to the web version of the article.)

there was no signal change after the non-complementary DNA reaction whereas the DPV signal of the MB decreased remarkably after hybridization with the target DNA.

The sensitivity of the pf-MWCNT WE based DNA sensor was investigated within 10 pM to 100 nM of the target concentration. The pf-MWCNT WEs were prepared by 30 s plasma treatment. Fig. 7(b) shows different peak currents obtained by the DPV signal of the MB after hybridization and Fig. 7(c) shows that the reduction current of the MB was linear with respect to the complementary DNA concentration over the whole range. The sensitivity was $-0.13688 \mu\text{A}/\text{M}$ with high regression coefficients ($R^2 = 0.9978$). For comparison, the 10 s plasma-treated MWCNT (10 s pf-MWCNT) based DNA sensor was also prepared and electrochemically measured in the same concentration range as the target DNA. We tried to prepare the pristine MWCNT based DNA sensor; however, the

probe DNAs were not effectively immobilized on the MWCNTs due to the lack of oxidative surface. The 10 s pf-MWCNT based sensor could detect the target in the concentration range of 100 pM to 100 nM with a sensitivity of $-0.05266 \mu\text{A}/\text{M}$ ($R^2 = 0.9472$). The sensitivity was lower, and the detection limit was worse than the 30 s pf-MWCNT based sensor. We concluded that the electrode with the larger effective area is directly related to the enhanced sensing performance such as sensitivity and the detection limit.

4. Conclusions

We successfully fabricated well-patterned MWCNT electrodes and a pf-MWCNT based electrochemical DNA sensor for *L. pneumophila* detection. A homogeneous MWCNT suspension and

transfer method could make MWCNTs possible to prepare the well-patterned MWCNT WEs, and from XPS and CV results we could conclude that the MWCNTs were effectively functionalized by oxygen plasma treatment. The plasma treatment of MWCNT WEs allowed higher electrocatalytic activity than pristine MWCNTs, and made the MWCNT surface induce oxygen-containing functional groups for covalently attachment to amine terminated probe DNA. Effective areas for MWCNT WEs were calculated from CV results, and their values of pf-MWCNT WEs were higher than pristine MWCNT WE. From a comparative study of 10 and 30 s (optimum condition) pf-MWCNT based DNA sensors, the higher effective area of WE value influenced sensitivity and the detection limit. DPV with pf-MWCNT WEs was optimized and successfully applied to DNA quantification of the *mip* sequence for *L. pneumophila* detection. Considering electrochemical results of electrodes themselves and DNA sensing performance, the pf-MWCNT WE presented here can be applied to other electrochemical biosensors since they have high electrochemical properties and the capability for easy functionalization.

Acknowledgement

This work was supported by grant no. K20601000002-07E0100-00210 from Korea Foundation for International Cooperation of Science & Technology.

References

- [1] S. Iijima, Nature 354 (1991) 56.
- [2] H. Cai, X.N. Cao, Y. Jiang, P.G. He, Y.Z. Fang, Analytical and Bioanalytical Chemistry 375 (2003) 287.
- [3] K. Min, Y.J. Yoo, Talanta 80 (2009) 1007.
- [4] J.X. Wang, M.X. Li, Z.J. Shi, N.Q. Li, Z.N. Gu, Electroanalysis 14 (2002) 225.
- [5] P.J. Britto, K.S.V. Santhanam, P.M. Ajayan, Bioelectrochemistry and Bioenergetics 41 (1996) 121.
- [6] M.L. Guo, J.H. Chen, D.Y. Liu, L.H. Nie, S.Z. Yao, Bioelectrochemistry 62 (2004) 29.
- [7] J.L. Bahr, J.M. Tour, Journal of Materials Chemistry 12 (2002) 1952.
- [8] A. Merkoci, M. Pumera, X. Llopis, B. Perez, M. del Valle, S. Alegret, Trac-Trends in Analytical Chemistry 24 (2005) 826.
- [9] T. Yang, W. Zhang, M. Du, K. Jiao, Talanta 75 (2008) 987.
- [10] N. Zhou, T. Yang, C. Jiang, M. Du, K. Jiao, Talanta 77 (2009) 1021.
- [11] T.M.H. Lee, L.L. Li, I.M. Hsing, Langmuir 19 (2003) 4338.
- [12] H.T. Fang, C.G. Liu, L. Chang, L. Feng, L. Min, H.M. Cheng, Chemistry of Materials 16 (2004) 5744.
- [13] Y.C. Xing, L. Li, C.C. Chusuei, R.V. Hull, Langmuir 21 (2005) 4185.
- [14] W. Zhao, H. Wang, X. Qin, X. Wang, Z. Zhao, Z. Miao, L. Chen, M. Shan, Y. Fang, Q. Chen, Talanta 80 (2009) 1029.
- [15] H. Yadegari, A. Jabbari, H. Heli, A.A. Moosavi-Movahedi, K. Karimian, A. Khodadadi, Electrochimica Acta 53 (2008) 2907.
- [16] J.X. Wang, M.X. Li, Z.J. Shi, N.Q. Li, Z.N. Gu, Microchemical Journal 73 (2002) 325.
- [17] H. Ago, T. Kugler, F. Caciagli, W.R. Salaneck, M.S.P. Shaffer, A.H. Windle, R.H. Friend, Journal of Physical Chemistry B 103 (1999) 8116.
- [18] N.P. Zschoerper, V. Katzenmaier, U. Vohrer, M. Haupt, C. Oehr, T. Hirtha, Carbon 47 (2009) 2174.
- [19] J.-Y. Lee, E.-J. Park, C.-J. Lee, S.-W. Kim, J.J. Pak, N.K. Min, Thin Solid Films 517 (2009) 3883.
- [20] K. Heuner, M. Swanson, Legionella Molecular Microbiology, Caister Academic Press, Norfolk, UK, 2008.
- [21] L. Fiume, M.A. Bucca Sabattini, G. Poda, Letters in Applied Microbiology 41 (2005) 470.
- [22] N.C. Engleberg, C. Carter, D.R. Weber, N.P. Cianciotto, B.I. Eisenstein, Infection and Immunity 57 (1989) 1263.
- [23] B. Ludwig, J. Rahfeld, B. Schmidt, K. Mann, E. Wintermeyer, G. Fischer, J. Hacker, FEMS Microbiology Letters 118 (1994) 23.
- [24] D.S.J. Lindsay, W.H. Abraham, R.J. Fallon, Journal of Clinical Microbiology 32 (1994) 3068.
- [25] D.A. Wilson, B. Yen-Lieberman, U. Reischl, S.M. Gordon, G.W. Procop, Journal of Clinical Microbiology 41 (2003) 3327.
- [26] B.M.W. Diederer, J. Kluytmans, C.M. Vandenberghe-Grauls, M.F. Peeters, Journal of Clinical Microbiology 46 (2008) 671.
- [27] F. Morio, S. Corvec, N. Caroff, F. Le Gallou, H. Drugeon, A. Reynaud, International Journal of Hygiene and Environmental Health 211 (2008) 403.
- [28] J. Amemura-Maekawa, F. Kura, B. Chang, H. Watanabe, Microbiology and Immunology 49 (2005) 1027.
- [29] Y. Jin, X. Yao, Q. Liu, J. Li, Biosensors and Bioelectronics 22 (2007) 1126.
- [30] A.J. Bard, L.R. Faulkner, Electrochemical methods: fundamentals and applications, 2nd ed., John Wiley & Sons, Inc., 2001.
- [31] S.-H. Zuo, L.-F. Zhang, H.-H. Yuan, M.-B. Lan, G.A. Lawrance, G. Wei, Bioelectrochemistry 74 (2009) 223.
- [32] G. Chen, D.H. Shin, S. Kim, S. Roth, C.J. Lee, Nanotechnology 21 (2010) 015704.

Eun Jin Park received her B.S. degree in biology from Chungnam National University, Korea in 2001 and her M.S. degree in molecular science technology from Aju University, Korea in 2003. She had worked as a researcher at BioChec. Inc., Korea from 2003 to 2004. She is currently pursuing her Ph.D. in the department of biomicrosystem technology at Korea University and has been doing so since 2005. Her areas of interest include electrochemistry, carbon nanotube based biosensors and DNA sensors.

Jun-Yong Lee received his B.S. degree in the department of control and instrumentation Engineering, Korea University in 2007. He is currently undertaking his Ph.D. course in the department of biomicrosystem technology. His interests include fabrication and electrochemical characterization of carbon nanotube films and carbon nanotube based biosensors and immunosensors.

Jun Hyup Kim received his B.S. degree in the department of control and instrumentation Engineering, Korea University in 2009. He is currently undertaking a Master's course in the department of biomicrosystem technology. His interests include fabrication and electrochemical characterization of carbon nanotube films and carbon nanotube based biosensors.

Cheol Jin Lee received the B.S. degree in electrical engineering (1982), and M.S. (1984) and Ph.D. (1993) degrees in electronic materials and devices, all from Korea University. He had worked as a senior researcher in the process development group of ULSI R & D, Samsung Electronics, Korea. He is currently a full professor in the school of electrical Engineering, Korea University. His current research interests include synthesis, characterization, purification, dispersion and functionalization of carbon nanotubes, and he is also interested in carbon nanotube based electronic devices.

H. Stanley Kim joined Korea University Medical College as an assistant professor in the spring semester of 2006, after 18 years of professional life in the United States of America. He is a microbial geneticist by training, and received his Master's and Ph.D. degrees from the department of microbiology, University of Illinois at Urbana-Champaign. He augmented and broadened his biological background during the postdoctoral years at Stanford University studying environmental microbiology and the newly conceived microarray technology, which was considered highly innovative at the time. In 2001, he moved to TIGR (The Institute for Genomic Research, Rockville, Maryland) and obtained hands-on experiences as a staff scientist conducting various functional genomic projects on cutting edge bioinformatics and genomics including those involving plant, bacterial, and fungal species. He remained a staff scientist at HIGR until 2006. His current interests include the genomics and bioinformatics of human pathogens, viral, bacterial, fungal and potential bio-warfare agents.

Nam Ki Min received the B.S. and M.S. degrees in electrical engineering from Korea University, Seoul in 1974 and 1976, respectively, and received his Ph.D. degree in electrical engineering from the University of Cincinnati, OH, USA in 1989. He is currently a full professor in the Department of Control and Instrumentation Engineering, Korea University, since 1989. His current research interests include nanobiosensors, MEMS-based sensors and smart sensor systems.